Journal of the Serbian Chemical Society
JSCS-info@shd.org.rs • www.shd.org.rs/JSCS
J. Serb. Chem. Soc. *82* (10) 1111–1121 (2017)
JSCS–5027
UDC 546.623'11'185:535.4–34:543.57+621.385.833
Original scientific paper

Effect of gamma-irradiation on the properties of aluminum dihydrogen triphosphate

WEIQIANG SONG[1]*, QINGHUAN SONG[2], LONGCHAO WU[1] and LANTAO YANG[1]

[1]*School of Materials Science and Engineering, Henan University of Technology, Zhengzhou 450001, China and* [2]*Medical Physics Laboratory, Luohe Medical College, Luohe 462003, China*

(Received 7 January, revised 15 July, accepted 17 July 2017)

Abstract: The effect of gamma irradiation on the properties of aluminum dihydrogen triphosphate (ADTP) in the dose range of 0 to 150 kGy was studied by X-ray diffraction (XRD) analysis, thermal analysis, acid–base titration, electrochemical impedance spectroscopy (EIS) and scanning electron microscopy (SEM). Although the XRD and SEM results indicated that there were no significant effects on the crystal structure and the surface morphology of ADTP, thermal analysis revealed that the crystal transition of $Al(PO_3)_3$ from Type-B to Type-A did not occur at a high temperature in irradiated ADTP. EIS results showed that high-dose gamma irradiation (100 kGy and 150 kGy, ^{60}Co) improved the corrosion inhibition ability of ADTP on tinplate steel. SEM was used to investigate the surface of tinplate steel panels after immersion in ADTP extracts for 69 h, and revealed that many slices were formed on the surface. The slices were attributed to the formation of $Fe_2P_3O_{10}$. Inter-slice gaps may be the reason for the lower corrosion resistance of ADTP compared with the resistance of some toxic pigments containing lead and chromium. Overall, high doses of gamma irradiation improved the corrosion resistance of ADTP.

Keywords: X-ray diffraction; thermal analysis; electrochemical impedance spectroscopy; scanning electron microscopy.

INTRODUCTION

The synthesis of aluminum dihydrogen triphosphate (ADTP) was first proposed by D'Yvoire in 1962,[1] and ADTP was structurally characterized by Rishi in 2006.[1,2] At present, ADTP is commercially available for industrial applications. One of the important applications of ADTP is in the field of anticorrosion coatings.

Traditional anticorrosive coatings contain lead or chromium(VI) compounds as active pigments due to their excellent cost/efficiency ratio. Due to the impo-

* Corresponding author. E-mail: weiqiang_song@haut.edu.cn
https://doi.org/10.2298/JSC170107090S

sition of increased legislative restrictions on the application of these toxic pigments containing lead or chromium, many compounds have been suggested as environmentally friendly alternatives.[3–6] One of the important alternatives is ADTP.[7–9] However, ADTP belongs to the solid acid group of compounds,[1,2] and therefore is usually considered to be less effective in the most widely used amine-cured epoxy coatings due to the reaction between ADTP and the amine hardeners and further to inferior storage stability. Several strategies have been developed to improve the performance of ADTP. However, the acidic nature of ADTP was verified to be retained after modification. For this reason, the present study was conducted to improve further the performance of ADTP by gamma irradiation.

A further reason for using gamma irradiation is its unique application in the modification of materials.[10–13] Gamma irradiation is a kind of green processing technology and an effective surface modification method with potential application prospects. However, the effect of gamma irradiation on ADTP was rarely reported in the relevant literature. In the present study, the primary aim was to investigate the effects of gamma irradiation on the structure and properties of ADTP, especially on electrochemical behavior in 3.5 % aqueous NaCl solution.

EXPERIMENTAL

Materials

In a typical procedure, aluminum hydroxide slurry and phosphoric acid solution (mole ratio of P_2O_5/Al_2O_3 is 3:1) were mixed at 90 °C in a container. The container was stirred at 100 °C for 1.5 h when the mixture turned into a translucent viscous slurry. The slurry was immediately placed into a reacting furnace set at 310 °C. After reacting for 10 h, the obtained solid was taken out of the furnace and immersed in distilled water. After hydration reaction, the product was treated by dehydration drying and further crushing. X-Ray diffraction (XRD) studies revealed the co-existence of two main structural phases, ADTP and $AlPO_4$, in the product. The product was not further separated and purified.

The product was divided into five portions. The portions sealed in polyethylene bags were subjected to total doses of 0, 20, 50, 100, and 150 kGy. A ^{60}Co gamma cell (7.4×10^{13} Bq) was used as a gamma ray source with a dose rate of 1 kGy h^{-1} at a temperature of 25 °C.

X-Ray diffraction

X-Ray diffraction spectra of non-irradiated and irradiated ADTPs (equilibrated at 100 % relative humidity, at 25 °C for 48 h) were recorded using an analytical diffractometer (Bruker D8 Advance), CuK_α radiation with a wavelength of 0.154 nm operating at 40 kV and 35 mA. XRD diffraction spectra were acquired at 25°C over a 2θ range of 5 to 80° with a step size of 0.02° and sampling interval of 10 s. The background was disregarded during analysis of XRD patterns.

Thermal analysis

Thermal behaviors of non-irradiated and irradiated ADTPs were studied by the simultaneous application of thermogravimetry (TG) and differential scanning calorimetry using a NETZSCH STA 409 PC/PG instrument. The samples were heated under a dynamic argon atmosphere, flow rate 30 ml min^{-1}, from room temperature to 1020 °C at a scan rate of 20 °C min^{-1} and the corresponding DSC and TG plots were obtained.

Titration experiment

Titration experiments were conducted to characterize the neutralizing ability of non-irradiated and irradiated ADTPs. The analyte was individually prepared by dissolving 0.2 g of non-irradiated and irradiated ADTPs in 20 mL of distilled water at 25 °C. The titrations were performed using a standard 0.05 mol L^{-1} NaOH titrant solution and a pH meter connected to a magnetic stirrer and pH electrode (E-201-9, Shanghai Yoke Instrument Co., Ltd.). Titrant increments of 1 mL and an equilibration time of 5 min were chosen.

Electrochemical measurements

The substrate consisted of tinplate steel (produced by Wuhan Iron and Steel (Group) Company), which was cut into test panels with dimensions 1 cm×1 cm×0.028 cm. The panels were pre-treated by mechanical cleaning (polishing), degreasing in an acetone solution and rinsing with distilled water. The backsides of the panels were electrically connected *via* a copper wire with a resin adhesive. In order to seal the edges and back sides, the panels were covered by the resin adhesive, leaving an apparent geometrical area of 1 cm^2 unmasked.

In order to prepare ADTP extracts, 0.2 g of each portion was stirred in 100 mL of 3.5 mass % aqueous NaCl solution for 24 h and then filtered after storing for 7 days at room temperature.

EIS measurements were performed in an RST5200F electrochemical workstation (Zhengzhou Shiruisi Instrument Technology Co., Ltd.) in the frequency range 100000 to 0.001 Hz using a perturbation amplitude of 5 mV around the open circuit potential. An electrochemical cell with a three-electrode configuration consisting of an Ag/AgCl reference electrode (RE), a panel as the working electrode (WE) and a platinum counter electrode (CE) was used for the measurements. Three replicate panels were conducted to ensure repeatability.

Surface analysis

The surface of the test panels after exposure to 3.5 % NaCl solution containing the ADTP extract was examined by scanning electron microscopy (SEM). Before the examination, the panels were washed with double distilled water and dried. An Inspect F50 scanning electron microscope operating at an accelerating voltage of 20 kV with a working distance of 18 mm was used.

RESULTS AND DISCUSSION

X-Ray diffraction pattern

The X-ray diffraction patterns of non- and irradiated ADTPs are shown in Fig. 1. The major peaks were assigned to $AlPO_4$ (JCPDS 45-0177 and 10-0423) and $AlH_2P_3O_{10}\cdot 2H_2O$ (JCPDS 31-0017), which indicated that the ADTP was a composite of $AlH_2P_3O_{10}\cdot 2H_2O$ and $AlPO_4$. Through comparison, it is clear that the spectra display no obvious difference in pattern characteristics of ADTPs irradiated at different doses, including the position and the amplitude of diffraction peaks, which suggests that no new crystalline phase existed in the irradiated ADTPs.

DSC and TG plots

To evaluate the gamma-irradiation effect on the thermal property of ADTP, TG and DSC analysis were performed. The TG curves and the corresponding DSC curves for ADTPs are shown in Figs. 2 and 3, respectively.

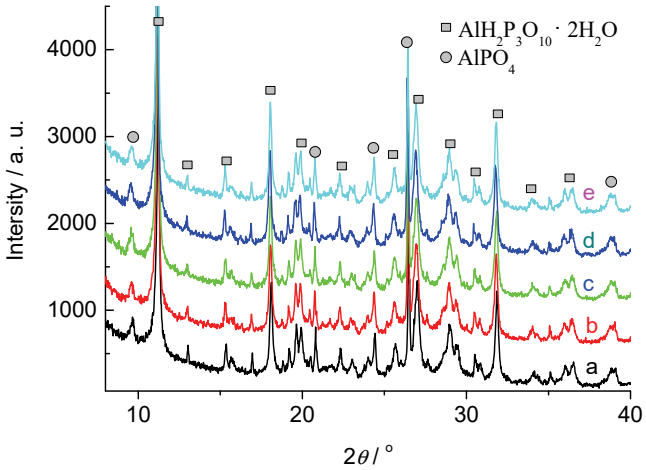

Fig. 1. X-Ray diffraction patterns of non-irradiated and irradiated ADTPs; a) non-irradiated and gamma-irradiated at: b) 20, c) 50, d) 100 and e) 150 kGy.

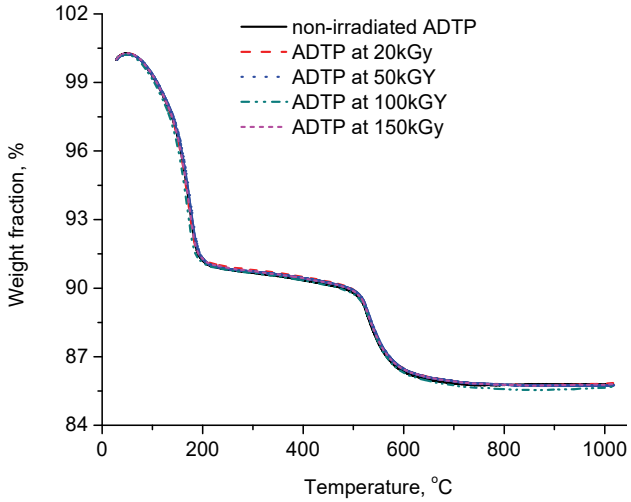

Fig. 2. TG curves for ADTPs non-irradiated and irradiated at 20, 50, 100 and 150 kGy.

The plots in Fig. 2 show water loss occurred in two steps. The first, with an associated thermal event at around 180 °C, corresponds to the loss of weakly bound water. There is no difference between the values of the loss for non-irradiated and irradiated ADTP, the values of which are close to 9.1 wt. %. The second at around 541 °C was associated with the loss of more tightly bound water, 4.0 wt. %. The dehydration processes are proposed as follows:

$$AlH_2P_3O_{10} \cdot 2H_2O \xrightarrow{135\text{–}195\ ^\circ C} AlH_2P_3O_{10} \xrightarrow{510\text{–}595\ ^\circ C} Al(PO_3)_3$$

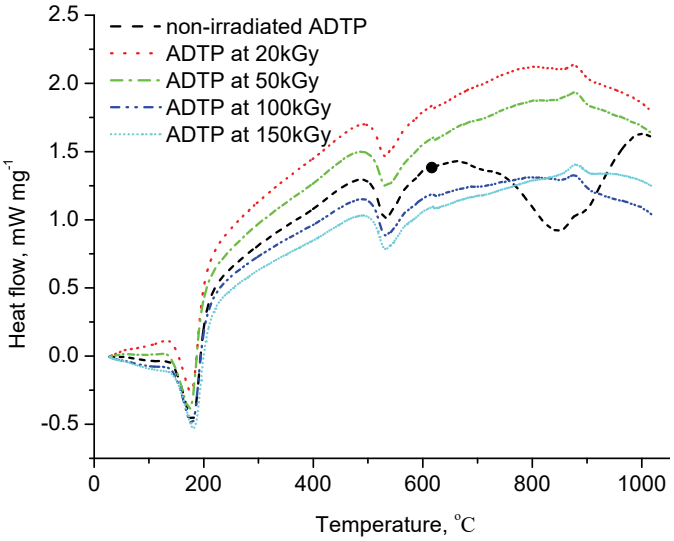

Fig. 3. DSC curves for ADTPs, non-irradiated and irradiated at 20, 50, 100 and 150 kGy.

More specifically, there was a significant thermal event in the temperature range of 750 to 990 °C for non-irradiated ADTP, as shown in Fig. 3, while there was no visible thermal event in the same temperature range for the irradiated ADTPs. However, in the corresponding temperature range on the TG curves, Fig. 2, there was no weight loss for the non-irradiated ADTP, which indicates that the thermal event could be attributed to phase transition. The following phase transition is proposed:

$$Al(PO_3)_3 \text{ (type-B)} \xrightarrow{750\text{–}970\ ^\circ C} Al\left(PO_3\right)_3 \text{ (type-A)}$$

This could be attributed to gamma irradiation causing a change in the structure of ADTP, and this change blocked the crystal transition. However, in view of the diffraction pattern shown in Fig. 1, all being the same, the change in the structure of ADTP cannot be a change in the crystal structure. Taking into account that water molecules easily decompose under gamma rays,[14] the change is attributed to the decomposition of the interlayer water molecules in the layered structure of ADTP.

Titration

ADTP is an acidic triphosphate and hence, the effect of gamma-irradiation on its acidity was investigated. The pH titration curves of saturated aqueous solutions of non-irradiated and irradiated ADTPs are shown in Fig. 4. The curves show an increase in the pH value from 4.4 to 12.0 on addition of OH^- for all the ADTP solutions.

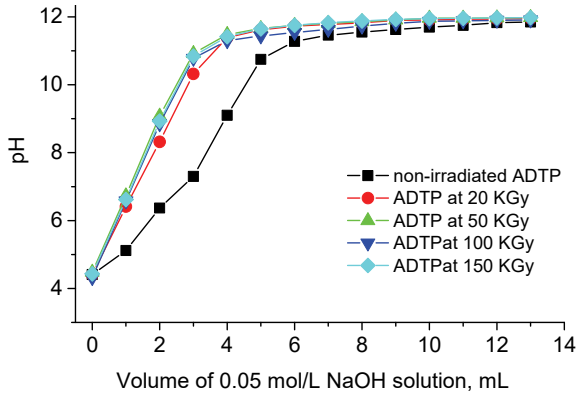

Fig. 4. pH titration curves of ADTP solutions.

However, as opposed to ZnO/SiO_2-modified ADTP pigment (ZnSi-ADTP),[15] gamma irradiation did not affect the acidity of the ADTP solutions, *i.e.*, all the initial solutions of the non-irradiated and irradiated ADTPs had the same pH value before titration, as shown in Fig. 4. Compared to ADTP, gamma irradiation in the dose range 20–150 kGy had a significant effect on the pH value of the initial solution of ZnSi-ADTP. The pH value of the initial solution of ZnSi--ADTP significantly increased from 4.9 to 9.4 with increasing absorbed dose from 0 to 150 kGy.[15]

Although gamma irradiation had no effect on the pH value of the initial solutions of ADTPs, the pH values of irradiated ADTPs solutions were higher than that of non-irradiated ADTP solution at the same dose of OH^- in the titration process.

Impedance measurements

ADTP is mainly used as an anticorrosion pigment. In order to evaluate the effect of gamma-irradiation on the anticorrosive property of ADTP, it was intended to reproduce its protection mechanistic stage when it is dispersed in the coating. According to the mechanism, 3.5 % NaCl solution was selected as the corrosive medium, an aqueous extract of ADTP was incorporated into it, and tinplate steel was used as the to be protected panel.

The Nyquist and Bode plots for tinplate panels obtained in ADTP extracts after immersion for 69 h are shown in Fig. 5. As shown in Fig. 5a, the Nyquist plot shows a single semicircle for tinplate panels in all the ADTP extracts. As shown in Fig. 5b, the slopes of Z in all the ADTP extracts in the middle range of frequency were close to –1, which demonstrates the same capacitive character. Presented on the Bode phase diagrams in Fig. 5c, the frequency at the maximum phase angle remained approximately at the same level when the absorbed dose of ADTP was increased from 0 to 150 kGy, which reveals that the capacitance on

the steel surface approximately remained unchanged in the investigated range of absorbed doses by ADTP.

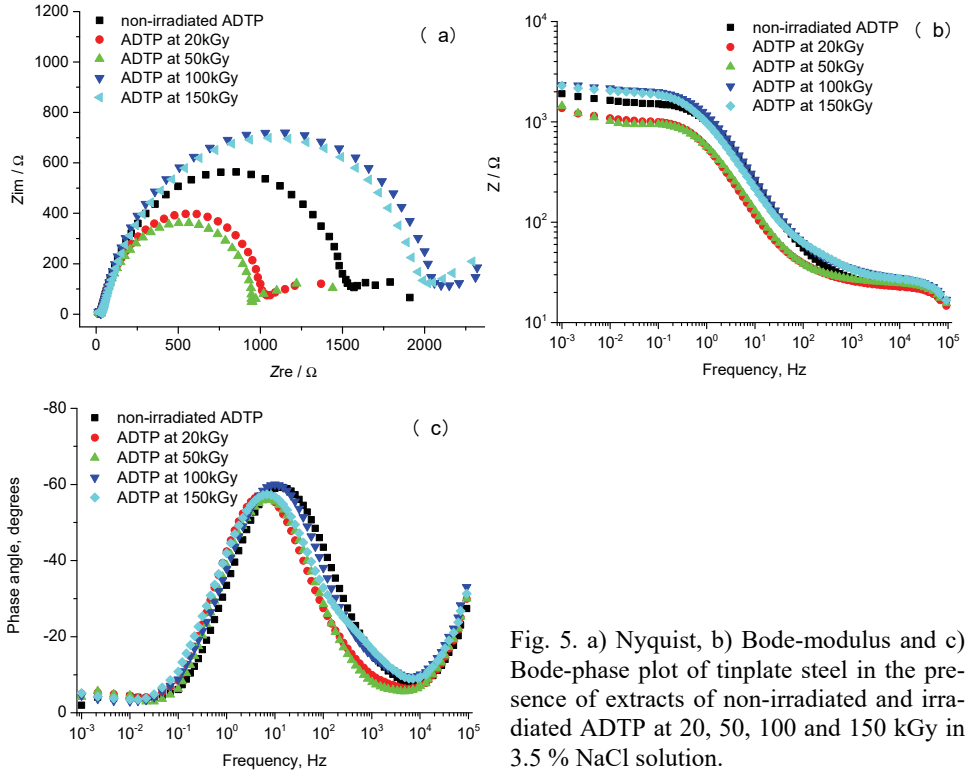

Fig. 5. a) Nyquist, b) Bode-modulus and c) Bode-phase plot of tinplate steel in the presence of extracts of non-irradiated and irradiated ADTP at 20, 50, 100 and 150 kGy in 3.5 % NaCl solution.

A single time constant represented by a single semi-circle was noticed for each of the tinplate steel panels, which could be simulated by the equivalent circuit shown in Fig. 6. Here, R_s represents solution resistance, C_{dl} the double layer capacitance at the interface between the protective layer and the panel substrate, R_{ct} the charge transfer resistance at the interface between the protective layer and the panel substrate, and W the impedance caused by diffusion process. R_{ct} is related to the charge transfer occurring due to the electrochemical reaction at the interface. As the value of R_{ct} can be obtained from the diameter of the Nyquist plot, a larger diameter indicates a higher resistance. It is clear from the plot, that the diameter of the semicircles increased in the order ADTP irradiated at 50, 20, 0, 150 and 100 kGy. Accordingly, the tinplate steel panels immersed in

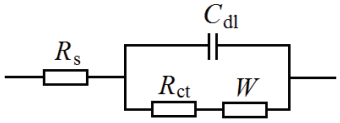

Fig. 6. The equivalent circuit used to model the experimental EIS data of tinplate steel in 3.5 % NaCl solution in the presence of non-irradiated and irradiated ADTPs.

the extracts of irradiated ADTPs at 100 and 150 kGy, displayed the maximal resistances.

SEM analysis

The SEM micrographs obtained for non-irradiated ADTP and 150 kGy--irradiated ADTP are shown in Fig. 7a and b, respectively. It is clear that gamma irradiation had no effect on the appearance and shape of ADTP, *i.e.*, ADTP still had a multi-layered structure after irradiation.

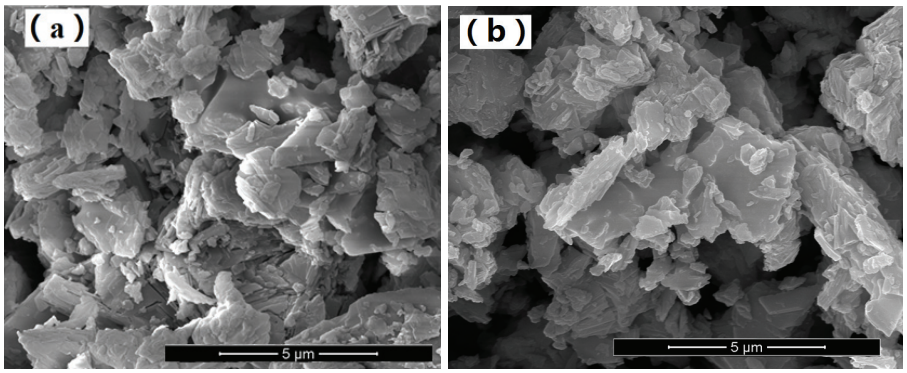

Fig. 7. SEM micrographs obtained for: a) non-irradiated ADTP and b) 150 kGy-irradiated ADTP.

For comparison, Figs. 8a–c shows the surface appearances of tinplate steel panels immersed in 3.5 % NaCl solution in the absence of ADTP extract, in the presence of non-irradiated ADTP extract and in the presence of 150 kGy--irradiated ADTP, respectively. Fig. 8a displays the polished metal surface of a tinplate steel panel. Figs. 8b and c reveal that there were pieces of protective film on the surface of tinplate steel panels, and that there were many gaps in the film.

ADTP belongs to the kind of condensed phosphates. In the literature,[16] the protective mechanism of ADTP for steel is proposed as follows: when it is dissolved in an aqueous solution, the triphosphoric ion ($P_3O_{10}^{5-}$) is formed, which exhibits a strong chelation ability and can chelate with various metal ions, such as ferrous iron and ferric iron. The protective film formed by the chelates on the metal surface is stable and can provide protective effect. When the triphosphoric ion is depolymerized, the formed orthophosphate ion (PO_4^{3-}) can also construct a protective film. Accordingly, the protective films displayed in Figs. 8b and c can be considered to be made of $Fe_2P_3O_{10}$. In addition, crystalline particles of $Fe_x(PO_4)_y$ were formed, which attached themselves to the protective film as shown in Figs. 8b and c:

$$AlH_2P_3O_{10} \rightarrow Al^{3+} + 2H^+ + P_3O_{10}^{5-}$$

$$Fe^{2+} + Fe^{3+} + P_3O_{10}^{5-} \rightarrow Fe_2P_3O_{10}$$

$$P_3O_{10}^{5-} + 2H_2O \rightarrow 3PO_4^{3-} + 4H^+$$

$$x\left(Fe^{2+},\ Fe^{3+}\right) + yPO_4^{3-} \rightarrow Fe_x\left(PO_4\right)_y$$

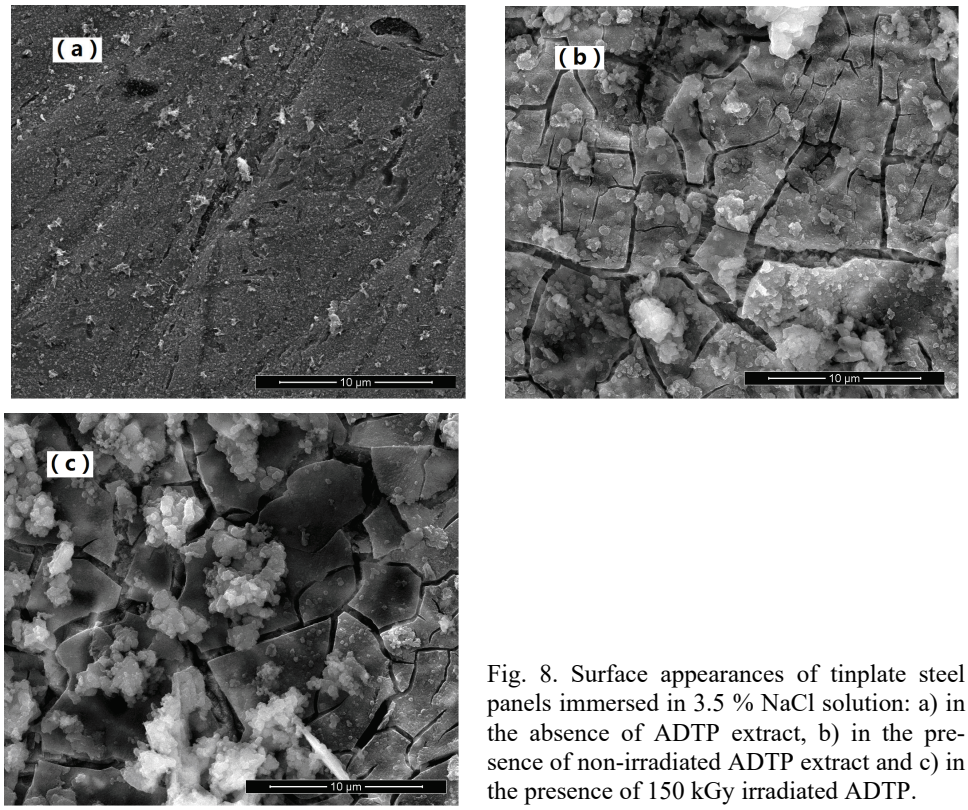

Fig. 8. Surface appearances of tinplate steel panels immersed in 3.5 % NaCl solution: a) in the absence of ADTP extract, b) in the presence of non-irradiated ADTP extract and c) in the presence of 150 kGy irradiated ADTP.

It is important to note that the steel substrate can be seen through the interslice gaps. In literature, alternative phosphate pigments did not quite match the high anticorrosive efficiency of lead or chromium(VI) compounds.[7] The presence of the interslice spacing may be the reason for the low corrosion resistance of ADTP.

CONCLUSIONS

Gamma-irradiation at doses up to 150 kGy caused no significant change in the crystal structure and appearance of ADTP, however, prevented the crystal transition of $Al(PO_3)_3$ formed at high temperature from Type-B to Type-A. According to the result of the titration experiment, the pH value of irradiated--ADTP solution was higher than that of non-irradiated-ADTP solution using the

same volume of 0.05 mol L^{-1} NaOH titrant, which was attributed to a decrease in acid group content in ADTP under gamma irradiation. Impedance measurements indicated that high doses of gamma irradiation were required in order to improve the corrosion inhibition ability of ADTP. SEM micrographs confirmed that pieces of a protective layer formed on the surface of tinplate panels in ADTP extracts, and further revealed that the layer was not a complete layer, but divided into many small pieces. The incomplete layer may be the cause of the decline in the corrosion inhibition ability of ADTP. Nevertheless, gamma irradiation at high doses improved the corrosion resistance of ADTP.

Acknowledgments. This study was supported by research project supported by the Natural Science Foundation of Henan Province (Grant No. 152102210069) and the Science and Technology Innovation Team Project of Zhengzhou City (Grant No. 131PCXTD615).

ИЗВОД

УТИЦАЈ γ-РАДИЈАЦИЈЕ НА СВОЈСТВА АЛУМИНИЈУМ-ДИХИДРОГЕН-ТРИФОСФАТА

WEIQIANG SONG[1], QINGHUAN SONG[2], LONGCHAO WU[1] и LANTAO YANG[1]

[1]*School of Materials Science and Engineering, Henan University of Technology, Zhengzhou 450001, China* и [2]*Medical Physics Laboratory, Luohe Medical College, Luohe 462003, China*

Применом методе дифракције рендгенских зрака (XRD), термалне анализе, ацидо–базних титрација, спектроскопије електрохемијске импеданције (EIS) и скенирајуће електронске микроскопије (SEM) испитиван је утицај γ-радијације при дози од 0 до 150 kGy на својства алуминијум-дихидроген-трифосфата (ADTP). Упркос чињеници да XRD и SEM резултати указују на то да не постоји значајан утицај на структуру кристала и морфологију површине ADTP, резултати испитивања на бази термалне анализе показују да у току γ-радијације на високим температурама не постоји трансформација кристала $Al(PO_3)_3$ из типа-A у тип-B. Резултати испитивања EIS методом су показали да је при високим дозама γ-радијације (100 и 150 kGy, ^{60}Co) побољшана корозиона инхибиторска способност ADTP на челичном лиму. Метода SEM је употребљена за испитивање површине панела челичног лима после потапања у раствор ADTP након 69 h, при чему је нађено да долази до формирања много слојева на површини лима, који највероватније потичу од $Fe_2P_3O_{10}$. Претпостављено је да празан простор између слојева може бити разлог слабије корозионе отпорности ADTP у односу на неке токсичне пигменте који садрже олово и хром. На крају, може се закључити да γ-радијација при високим дозама доприноси повећаној корозионој отпорности ADTP.

(Примљено 7. јануара, ревидирано 15. јула, прихваћено 17. јула 2017)

REFERENCES

1. P. Thomas, *Studies into the ion exchange and intercalation properties of $AlH_2P_3O_{10}\cdot 2H_2O$*, University of Birmingham, Birmingham, 2011
2. S. K. Rishi, B. M. Kariuki, N. J. Checker, J. Godber, A. J. Wright, *Chem. Commun*. **37** (2006) 747
3. S. Alinejad, R. Naderi, M. Mahdavian, *Prog. Org. Coat*. **101** (2016) 142
4. S. Chen, M. Cai, X. Ma, *J. Alloys Compd*. **689** (2016) 36
5. M. J. Gimeno, M. Puig, S. Chamorro, J. Molina, R. March, E. Oró, P. Pérez, J. J. Gracenea, J. J. Suay, *Prog. Org. Coat*. **95** (2016) 46

6. N. Malatji, A. P. I. Popoola, O. S. I. Fayomi, C. A. Loto, *Int. J. Adv. Manuf. Technol.* **82** (2016) 1335
7. M. Deyá, V. F. Vetere, R. Romagnoli, B. del Amo, *Pigm. Resin Technol*. **30** (2001) 13
8. D. Song, J. Gao, L. Shen, H. Wan, X. Li, *J. Chem-NY* **2015** (2015) 1
9. X. Lu, Y. Zuo, X. Zhao, Y. Tang, *Electrochim. Acta* **93** (2013) 53
10. A. Sudha, T. K. Maity, S. L. Sharma, *Mater. Lett*. **164** (2016) 372
11. D. Guo, X. Zu, G. Yang, J. Huang, F. Wang, H. Liu, X. Xiang, X. Jiang, *Opt. Mater*. **54** (2016) 238
12. M. A. Ouis, H. A. Elbatal, A. M. Abdelghany, A. H. Hammad, *J. Mol. Struct*. **1103** (2016) 224
13. S. Sadhasivam, N. P. Rajesh, *Mater. Res. Bull*. 7**4** (2016) 117
14. Y. Wada, K. Kawaguchi, M. Myouchin, *Prog. Nucl. Energy* **29** (1995) 251
15. W. Song, K. Niu, L. Wu, *Radiat. Eff. Defects Solids* **5**–**6** (2016) 1
16. C. Yun, *China Coat.* **22** (2007) 19.